AN ELECTRON BEAM DIAGNOSTIC FOR THE LOS ALAMOS FREE-ELECTRON LASER OSCILLATOR EXPERIMENT*

R. L. Sheffield, AT-7, MS-H825
Los Alamos National Laboratory, Los Alamos, New Mexico 87545 USA

Summary

An electron beam diagnostic for the Los Alamos free-electron laser (FEL) oscillator experiment has been used to measure the time dependence of the electron energy distribution in a 100-μs time interval. The electron beam consists of macropulses that have a duration of 100 μs and a repetition rate of 1 Hz. Each macropulse consists of a series of micropulses that have ∿30 ps duration, ∿50 A peak current, and ∿50 ns separation. The primary purpose of the electron beam diagnostic is measurement of the time dependence of the electron energy distribution during the build-up of the photon field in the oscillator. Since the exact time of build-up depends on various rf and cavity considerations, provisions were made to allow the observation window to be varied from 10 to 100 μs and to be delayed by times up to 100 μs.

Introduction

In contrast to the Los Alamos FEL amplifier experiment,[1,2] where operation of a FEL at moderate to high signal level was simulated for a few nanoseconds, the Los Alamos FEL oscillator[3,4] experiment allows observation of the optical and electron beam energy over a much larger range of optical signal level, that is, from spontaneous emission to gain saturation. This paper describes an electron beam diagnostic developed to determine the details of the electron energy distribution during the evolution of the optical signal. In addition, the electron beam diagnostic is used to facilitate the tuning and operation of the gun pulser, subharmonic bunchers, and the accelerator tanks.

The electron beam is derived from a pulsed triode gun that produces a macropulse consisting of a train of pulses 5 ns in duration separated by ∿50 ns. This electron beam is subsequently bunched and accelerated to a nominal 20-MeV energy. The temporal characteristics, shown in fig. 1, of the resultant beam are macropulses with a duration of 100 μs and a 1-Hz repetition rate. Each macropulse contains a series of micropulses of 30-ps duration separated by 50 ns. The peak current in the micropulses is ∿50 A.

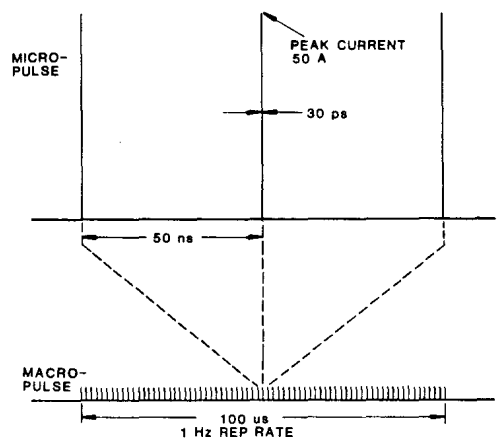

Fig. 1. Temporal characteristic of the macropulse.

*Work performed for Defense Advanced Research Projects Agency under the auspices of the US Department of Energy.

The experimental configuration downstream from the wiggler is shown in fig. 2. The first component is the slow deflector. The purpose of the slow deflector is to deflect the beam vertically during the macropulse and thereby produce a display of the time history of the electron energy distribution on the quartz view screen for a macropulse. Next in the beamline is the fast-deflector cavity. This is an rf cavity[5] operating in the TM_{110} mode, that is, with horizontal magnetic fields on the beam axis. As with the slow deflector, these fields deflect vertically and produce a display of the time history on a micropulse time scale. Following the fast deflection cavity are the diagnostic quadrupole, the spectrometer magnet, and the quartz view screen. The quartz screen is viewed by gateable microchannel-plate (MCP) intensified vidicon cameras. The MCP intensifiers are electrically gated to allow the isolation of a single micropulse.

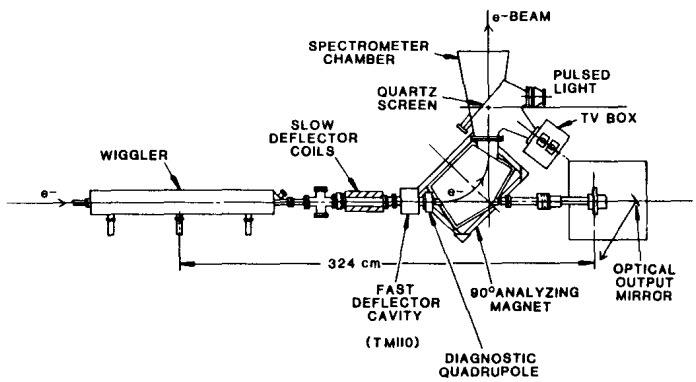

Fig. 2. Electron beam-diagnostic apparatus.

Slow-Deflector Coil

The slow deflector ramps the electron beam macropulse on the quartz target to display the energy distribution as a function of time. The slow deflector consists of two coils connected in parallel and mounted on a thin stainless steel tube. The peak field is 90 G. An aluminum tube surrounds the coil, providing structural support and magnetic shielding for containing the deflector fields.

The slow-deflector coil drive produces a trapezoidal current waveform. The integrated voltage (proportional to the magnetic field) induced in a flux loop positioned in the center of the coil is shown in fig. 3. The two flat portions of the trace correspond to the electron beam being "parked" so as not to impact chamber walls, eliminating the need for extra shielding. The sloped portion of the trace corresponds to the sweep across the quartz target. Either parking current can last from 0 to 100 μs and the sweep duration can be varied from 10 to 100 μs. The inductance of the 30-cm-long coil is 3.5 μH. The peak drive is +100 A at +100 V to -100 A at -100 V.

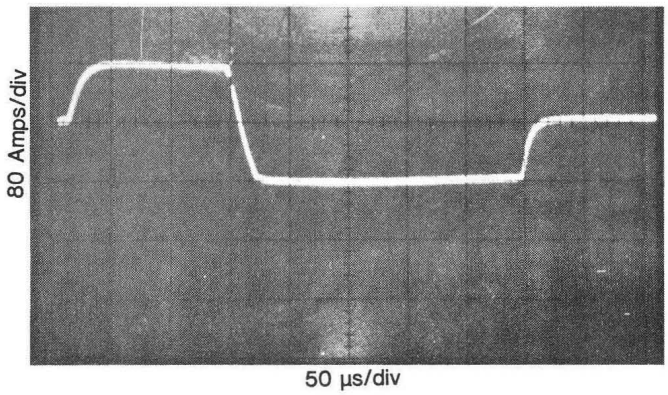

Fig. 3. Schematic of beam deflection by the slow deflector.

The deflection plane is vertical (the spectrometer energy dispersion is horizontal). With laser light present, the evolution of electron energy and momentum losses can be followed from spontaneous emission to laser saturation, shown schematically in fig. 4. With no laser present, the energy dispersion versus time characterizes accelerator and buncher operation. The diagnostic is then used as a performance monitor to optimize gradients and phasing of the accelerator and buncher.

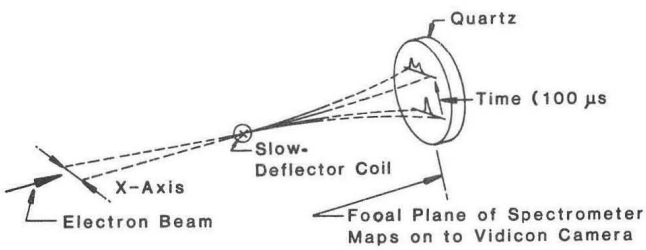

Fig. 4. Magnetic field as a function of time inside the slow deflector.

Diagnostic Quadrupole

A quadrupole is inserted just upstream of the magnetic spectrometer (see fig. 2). This quadrupole serves two purposes. First, it can adjust the axial position of either the vertical or horizontal beam waist at the target screen (fig. 5) to allow maximizing either vertical (time) resolution or horizontal (energy) resolution without affecting the experimental configuration. Second, the quadrupole shifts the effective deflection point of both the slow and fast deflectors in a manner that increases the vertical deflection at the target screen, thus giving better vertical resolution. The vertical centroid shift of the electron beam from the undeflected position is given as a function of quadrupole field in fig. 6.

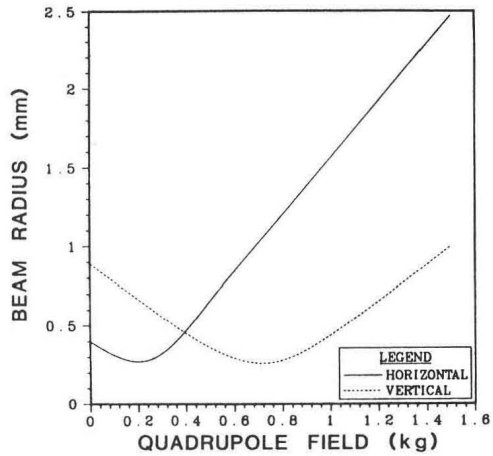

Fig. 5. Calculated electron beam radius at quartz screen as a function of quadrupole field. Actual beam radius is approximately twice as large because of beam emittance.

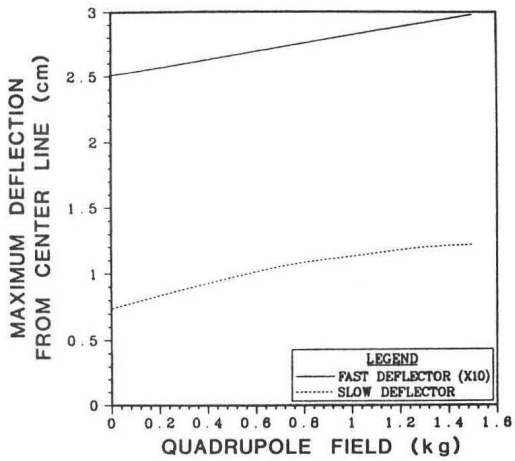

Fig. 6. Vertical deflection as a function of quadrupole field for both deflectors at quartz screen.

Gated Microchannel-Plate Camera

A gated MCP intensified vidicon camera provides time discrimination between individual micropulses and is capable of selecting and amplifying a single micropulse out of the pulse train and of providing data to maximize the peak current. In the presence of a laser field, the energy spread of a single micropulse can be measured from onset of oscillation to saturation.

The cameras view a quartz target. The observed light from the beam interacting with the target is due to Cerenkov radiation. Because quartz has essentially no fluorescence tail, the light from one micropulse will not overlap (in time) with light from any other pulse.

Two MCP vidicon cameras view the quartz screen. One camera with a wide field of view is used with the slow deflector. The other camera with a smaller field of view (greater magnification) is used with the fast and slow deflectors. The overall resolution is limited by the beam spot size and not by the camera system. For the slow deflector, the maximum deflection is 2.0 cm. At the minimum vertical waist of 1.0 mm, the resolution is 20. (Resolution is defined as deflection divided by spot size).

Experimental Results

The primary purpose of this diagnostic is to monitor changes in the electron energy spectrum caused by laser oscillation. The uncorrected electron energy spectrum without oscillation is shown in fig. 7. Qualitative effects in the data can be shown by using image processing techniques to produce a psuedo 3D image (fig. 8). For quantitative measurements, a Nicolet Model 2090 oscilloscope is used to display individual television raster lines. The slow deflector correlates raster lines to time during the macropulse. Any raster line may be selected for display on the Nicolet; therefore, the electron energy spread may be displayed for any point in time of the macropulse. Figure 9(a) and 9(b) are individual raster lines without and with oscillation, respectively. Integrating over energy for each of the raster lines gives a beam energy decrease of 0.3 to 0.4% because of oscillation. This diagnostic is also used to monitor beam buncher and accelerator performance. The phase between and gradients of the buncher and accelerators have pronounced effects on the energy versus time presentation. Difficulties in beam operation result in energy oscillation and energy slope, as well as variations in beam energy spread over the duration of the macropulse.

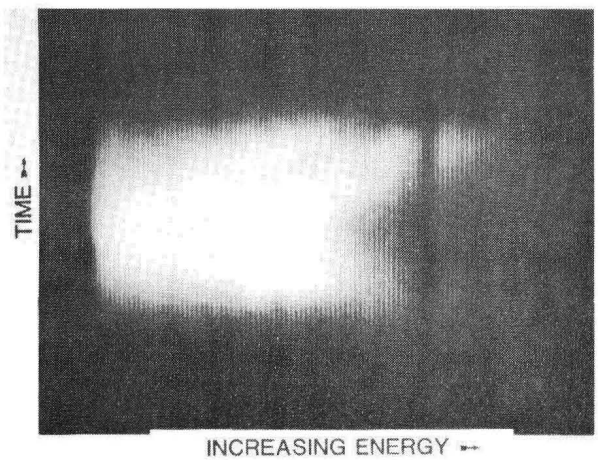

Fig. 7. Photograph of uncorrected data. Picture shows electron-beam-generated Cerenkov light in quartz slabs 0.5 mm thick. Dark line in middle of pattern are slab edges that have been coated with graphite.

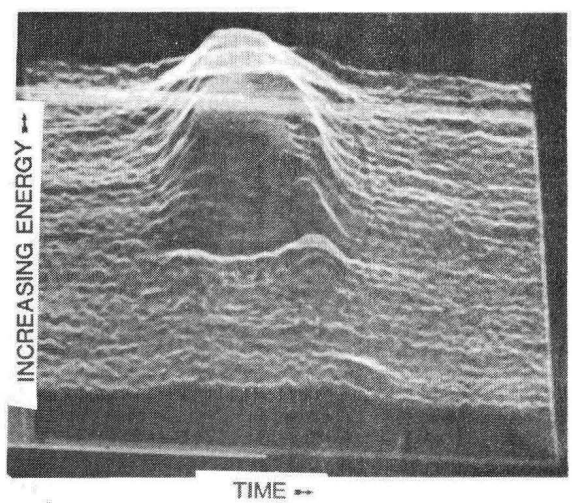

Fig. 8. Psuedo 3D image of fig. 7. Relief corresponds to intensity.

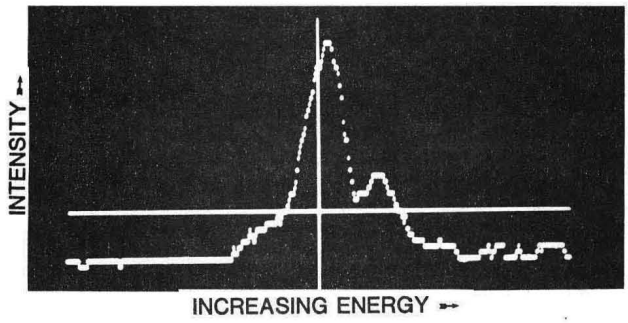

(a)

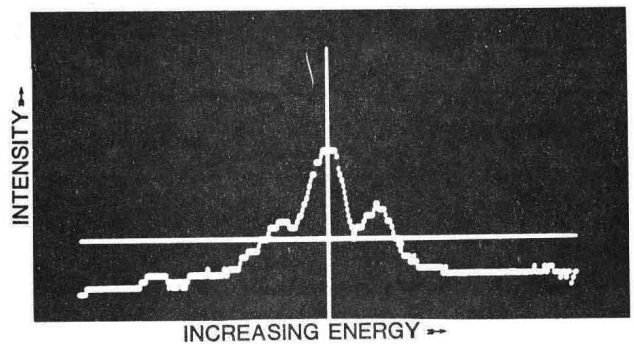

(b)

Fig.9. Single raster scans through data in the form of fig. 7. Traces (a) and (b) correspond to electron beam energy spread without and with laser oscillation, respectively.

References

1. R. W. Warren, B. E. Newnam, J. G. Winston, W. E. Stein, L. M. Young and C. A. Brau, "Results of the Los Alamos Free-Electron Laser Experiment," IEEE J. Quantum Electron, QE-19, 391 (1983).

2. B. E. Newnam, K. L. Hohla, R. W. Warren and J. C. Goldstein, "Optical Diagnostics for the Los Alamos Free-Electron Laser Amplifier Experiment," IEEE J. Quantum Electron, QE-17, 1480 (1981).

3. R. W. Warren, J. S. Fraser, W. E. Stein, J. G. Winston, T. A. Swann, A. Lumpkin, R. L. Sheffield, J. E. Sollid, B. E. Newnam, C. A. Brau and J. M. Watson, "The Los Alamos Free-Electron Laser Oscillator Experiment: Plans and Present Status," SPIE Proc. Free-Electron Generators of Coherent Radiation 453, 130 (1983).

4. R. W. Warren, B. E. Newnam, W. E. Stein, J. G. Winston, R. L. Sheffield, M. T. Lynch, J. C. Goldstein, M. C. Whitehead, O. R. Norris, G. Luedemann, T. O. Gibson, and C. M. Humphry, "First Operation of the Los Alamos Free-Electron Laser Oscillator," in Proc. Int. Conf. on Laser '83, to be published, 1984.

5. R. L. Sheffield, W. E. Stein, A. Lumpkin, R. W. Warren, and J. S. Fraser, "Electron Beam Diagnostics for the Los Alamos Free-Electron Laser Oscillator Experiment," SPIE Proc. Free-Electron Generators on Coherent Radiation 453, 151 (1983).